

## Methylene blue adsorption on *Parinari excelsa* biochar in aqueous solution

John Mambu Koroma<sup>a</sup>, Kaibo Pu<sup>a</sup>, He Zhang<sup>a</sup>, Jirui Bai<sup>a</sup>, Mohamed Sidi Almouctar<sup>b</sup>, Yunhai Wang<sup>a,\*</sup>

<sup>a</sup>Department of Environmental Science and Engineering, School of Energy and Power Engineering, Xi'an Jiaotong University, Xi'an, Shaanxi Province 710049, China, emails: wang.yunhai@mail.xjtu.edu.cn (Y. Wang), johnkoroma2013@gmail.com (J.M. Koroma), 1483484501@qq.com (K. Pu), zhanghezixian@qq.com (H. Zhang), 582097953@qq.com (J. Bai)

<sup>b</sup>Department of Earth and Environmental Science, School of Human Settlements and Civil Engineering, Xi'an Jiaotong University, Xi'an, Shaanxi province 710049, China, email: sidialmouctarp@gmail.com

Received 17 September 2020; Accepted 26 June 2021

### ABSTRACT

Methylene blue (MB) dye, similar to many modern dyes, poses environmental problems. *Parinari excelsa* is a large tropical tree that is common in many parts of humid Africa and tropical South America. In this study, biochar prepared from *P. excelsa* wood waste was characterized. Batch studies were conducted to determine the MB adsorption efficiency of the *P. excelsa* biochar. The MB adsorption efficiency increased with increasing the contact time, biochar dosage, pH and sodium chloride concentration. Also the percentage uptake decreased with increasing the initial concentration of MB solution. The adsorption equilibrium data were fitted with Langmuir, Freundlich, Temkin and D-R isotherm models. The analysis showed that the Langmuir model showed the best isotherm fit, while the adsorption kinetics was best described by pseudo-second-order kinetic model. The adsorption mechanism was described as physisorption. The adsorption capacity of 30 mg/g was estimated and the equilibrium was obtained within 720 min by removing 97% of MB from the aqueous solution. This research confirmed that *P. excelsa* biochar would serve as an effective adsorbent for the uptake of MB in aqueous solution.

*Keywords:* Adsorption; Isotherm; Kinetics; Methylene blue; *Parinari excelsa*

### 1. Introduction

Industries using dyes (e.g., paper, plastic, paint, and textile industries) are increasingly being set up in countries with weak enforcement of environmental regulations. Wastes from these industries are often discharged directly into aquatic environments with little or no processing [1]. Contamination of drinking water is a growing public health concern, particularly in poor communities in Sub-Saharan Africa [2–4]. Water pollution by industrial effluents is unsightly and disrupts photosynthesis in aquatic ecosystems [5,6]. More importantly, dyes and their metabolites can be

toxic, mutagenic or carcinogenic [7]. Therefore, the removal of these effluents from water bodies is critical.

The techniques for dye wastewater treatment include ion exchange [7], magnetic separation [8], dialysis [9], filtration, ultra-filtration [10,11] and flocculation [12]. These methods may usually have the disadvantages such as high cost, pollutant specific and less efficient in dye removal [13].

Because it is simple and cheap, adsorption is one of the main dye wastewater treatment technologies [13–15]. The porous structure, pore distribution and functional groups on the adsorbents are the main characteristics that drive the adsorption mechanism [10]. Biochar is a solid carbon product from pyrolysis of biomass materials. It can be

\* Corresponding author.

produced under different conditions for specific applications including carbon sequestration, soil amendment and environmental remediation [16,17]. A range of biochars have been fabricated and investigated for the cost-effectiveness and sustainability [18–20].

*Parinari excelsa* is a fast-growing tree that is commonly used in the production of charcoal across Africa (including Sierra Leone) and South America. *Parinari excelsa* contains various organic compounds (lignin, cellulose and hemicellulose) with polyphenolic and hydroxyl groups that may be useful in binding dyes via some complex mechanisms. The objective of this study was to develop a low-cost adsorbent for color removal from dye wastewater and study the adsorption kinetics. The MB was selected as a model dye as a result of its toxicity to humans and aquatic organisms [21]. *Parinari excelsa* has not been studied as biochar adsorbent for dye removal to our best knowledge. Preparing *P. excelsa* wood waste biochar to treat dye wastewater can be developed into a critical use pathway of biomass resources to solve water pollution within poor communities in Sub-Saharan Africa. Thus in this study, *P. excelsa* wood waste was pyrolyzed and the resulting biochar was used to remove MB from simulated wastewater. The adsorption capacity and kinetics of *P. excelsa* biochar were tested for the removal of MB.

## 2. Materials and methods

### 2.1. Materials

The woody biomass by-product or waste was collected from normal traditional farm brushes in the southern Sierra Leone, West Africa. Then the MB and other chemicals used in the experiment were procured from the Tianjin Damao Chemical Company in China, and the chemicals were of analytical grade.

#### 2.1.1. Adsorbent

The collected *P. excelsa* wood waste was cut into small pieces (1–2 cm long) and sun-dried for 2 weeks to get rid of the water content. The sample was milled into fine powder and sieved via 75-micrometer sieve in the laboratory to obtain uniform size. The ground biomass sample was pyrolyzed in a tube furnace without any pretreatment. The pyrolysis temperature of 700°C, residence time of 1 h, heating rate of 10°C/min and nitrogen flow rate of 0.4 L/min was used during the pyrolysis. Pyrolysis is one of the major thermal methods utilized to convert organic waste into carbon-rich material, which can be used for wastewater treatment [22]. During the pyrolysis process, cellulose, hemicellulose and lignin, which are the building blocks of biomass, are broken down under oxygen-limited conditions to enrich the carbon content of the original biomass [23]. Pyrolyzing biomass at high temperatures may increase the hydrophobicity, surface area and micropore volume [24], which may enhance the biochar adsorption performance. The biochar yield was ca. 28% under the above conditions.

#### 2.1.2. Adsorbate

A stock solution of 1,000 mg/L of MB was prepared by dissolving the appropriate dry mass of MB into deionized

water. The molecular formula of MB is  $C_{16}H_{18}N_3SCl$  with the molecular structure shown in Fig. 1. The experimental concentrations were prepared by successive dilution of the stock to a range of 25–75 mg/L using deionized water.

### 2.1.3. Biochar characterization

The surface characteristics (e.g., pore size, specific surface area and pore size distribution) were determined using SSA-4000 analyzer (Builder, China) following the BET method. The Fourier transforms infra-red (FTIR) spectrophotometer (Shimadzu-8400S, Japan) was used to determine the presence of different functional groups on the adsorbents. The FTIR of the adsorbent was examined before and after MB adsorption. The FTIR spectrum was recorded within the wavenumber range of 4,000–400  $cm^{-1}$ . The morphology and texture of the adsorbent before adsorption were analyzed using scanning electron microscopic (SEM, PHENOM ProX G6, Thermo Fisher Scientific, USA).

### 2.2. Batch adsorption experiment

In this study, batch adsorption of MB onto *P. excelsa* biochar was conducted as explained in the literature [25]. The effect of contact time was determined by adding 0.2 g *P. excelsa* biochar in 100 mL MB aqueous solution of 25 mg/L in a beaker placed in an intelligent magnetic water bath agitated at 150 rpm at 30°C, pH 7. The pH was adjusted with drops of 0.1 M HCl or NaOH. After adsorption test, solutions were filtered via Whatman® #42 filter paper to separate carbon from the solution and the residual MB concentration was determined using visible ultra-violet spectrophotometer (UV-3802, Unico, USA) at the wavelength of 665 nm.

The effect of adsorbent dose was determined by stirring 100 mL MB solution of 25 mg/L with *P. excelsa* biochar dosages ranging from 0.04 to 0.2 g. The effect of initial concentration was analyzed by stirring 0.2 g of *P. excelsa* biochar with MB concentrations ranging from 35 to 75 mg/L. The salinity effect was analyzed by adding sodium chloride in 100 mL solution with MB initial concentration of 35 mg/L.

The adsorption capacity of *P. excelsa* biochar at given equilibrium and adsorption efficiency was calculated using a standard equation [26]. The calibration curve for MB was prepared by measuring the absorbance of different MB concentrations at 665 nm [1]. The experimental parameters including the pH, contact time, initial concentration of adsorbent, adsorbent dose and ionic strength were investigated. For these investigations, each data point was the average for at least three repeated experimental data. The quantity of dye adsorbed at equilibrium was calculated as Eq. (1):

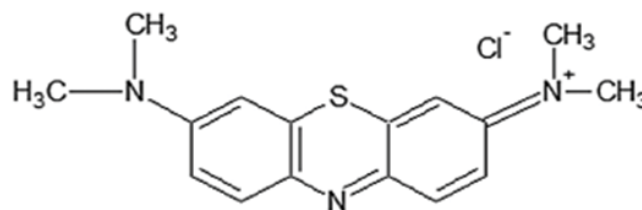


Fig. 1. Molecular structure of MB.

$$q_e = \frac{(C_0 - C_e)V}{W} \tag{1}$$

The efficiency of the adsorbent was calculated by Eq. (2):

$$\text{Removal of MB} = \frac{(C_0 - C_e)}{C_0} \times 100\% \tag{2}$$

Then the quantity adsorbed at the time  $t$  was calculated as Eq. (3):

$$q_t = \frac{(C_0 - C_t)}{W} \tag{3}$$

where  $C_0$ ,  $C_e$  and  $C_t$  (mg/L) are the concentrations at initial, equilibrium and time  $t$  (min) conditions, respectively;  $V$  (L) is the volume of the solution;  $W$  (g) is the dry mass of the adsorbent;  $q_e$  (mg/g) is the amount of dye adsorbed per mass of adsorbent at equilibrium; and  $q_t$  (mg/g) is the amount of dye adsorbed per mass of adsorbent at time  $t$ .

### 2.3. Adsorption mechanism and kinetics

The equilibrium isotherm of MB was examined by using different MB concentrations ranging from 35 to 75 mg/L and 0.2 g *P. excelsa* biochar and agitated at 150 rpm for 24 h to achieve equilibrium. The dye solution pH was adjusted to pH 7.

The adsorption mechanism was tested by fitting the dye equilibrium concentrations ( $C_e$ ) and the amount of dye adsorbed per mass of adsorbent at equilibrium ( $q_e$ ) to the Langmuir, Temkin and Dubinin–Radushkevich (D-R) adsorption isotherm models, respectively. Kinetic studies were conducted in a similar mode as the equilibrium test. For this investigation, a beaker containing 100 mL MB aqueous solution of 25 mg/L was agitated at 150 rpm, a portion of the MB aqueous solution was withdrawn from the beaker at a predetermined time and the concentration of MB was measured. The quantity of dye adsorbed at any given time  $q_t$  was determined using Eq. (3). The equilibrium data were fitted with pseudo-first-order, pseudo-second-order kinetic and Elovich models, respectively.

#### 2.3.1. Adsorption isotherm models

The Langmuir isotherm model is given as Eq. (4):

$$\frac{C_e}{q_e} = \frac{1}{Q_0 b} + \frac{C_e}{Q_0} \tag{4}$$

where  $C_e$  is the concentration of the adsorbate at equilibrium (mg/L);  $q_e$  is the amount of dye adsorbed per mass of adsorbent at equilibrium (mg/g);  $b$  and  $Q_0$  are the Langmuir constants related to the rate of adsorption and the adsorption capacity, respectively. When  $C_e/q_e$  is linearly plotted against  $C_e$ , with a slope  $1/Q_0$  and intercept  $1/Q_0 b$  is obtained.

The key characteristic of the Langmuir isotherm is called the separation factor  $R_L$  [27], which describes the nature

and characteristics of the adsorption process, is given by Eq. (5) as follows:

$$R_L = \frac{1}{(1 + bC_0)} \tag{5}$$

where  $C_0$  is the initial concentration of dye (mg/L); and  $b$  is the Langmuir constant. The value of  $R_L$  denotes the nature of the adsorption process, as in Eq. (5).

The logarithmic form of Freundlich isotherm is given as Eq. (6):

$$\log q_e = \log K_F + \frac{1}{n} \log C_e \tag{6}$$

The plot of  $\log q_e$  against  $\log C_e$  gives a straight line with a slope of  $1/n$  and intercept of  $\log K_F$ ; where  $K_F$  is the adsorption capacity of the adsorbent and  $n$  interprets the nature of the adsorption. The adsorption process is more heterogeneous when the slope  $1/n$  equals zero.

The linear form of the Temkin isotherm is given as Eq. (7):

$$q_e = \frac{RT(\ln a_T)}{b_T} + \frac{RT(\ln C_e)}{b_T} \tag{7}$$

where  $q_e$  (mg/g) is the amount of dye adsorbed per mass of adsorbent at equilibrium;  $b_T$  (mg/L) is the Temkin isotherm constant related to the energy parameter; and  $a_T$  (L/g) is the Temkin isotherm constant. The values of these constants are calculated from the slope and intercept obtained from the fitted plot of  $q_e$  against  $\ln C_e$ .

The linearized equation of the D-R isotherm is stated as Eqs. (8) and (9):

$$\ln q_e = \ln q_s - K\varepsilon^2 \tag{8}$$

$$\varepsilon = RT \ln \left( 1 + \frac{1}{C_e} \right) \tag{9}$$

where  $q_e$  and  $q_s$  are the equilibrium adsorbent-phase concentration of adsorbate and theoretical saturation capacity (mg/g), respectively;  $K$  is the D-R isotherm constant, related to the free energy of adsorption per mol of adsorbate ((mol/kJ)<sup>2</sup>); and  $\varepsilon$  is the Polanyi potential.

The adsorption free energy  $E = \frac{1}{\sqrt{2K}}$  provides an idea about the physical or chemical adsorption mechanism. If  $E$  is between 8 and 16 kJ/mol, the process of sorption is chemically driven, while if  $E$  is lower than 8 kJ/mol, then it is a physical process [26].

#### 2.3.2. Kinetic study

Pseudo-first-order, pseudo-second-order and Elovich models were used to analyze the kinetic data. These models can be expressed as Eqs. (10)–(12):

Pseudo-first-order:

$$\ln(q_e - q_t) = \ln(q_e) - K_1 t \tag{10}$$

Pseudo-second-order:

$$\frac{t}{q_t} = \frac{1}{K_2 q_e^2} + \frac{t}{q_e} \quad (11)$$

Elovich model:

$$q_t = \frac{1}{\beta} (\ln \alpha \beta) + \frac{1}{\beta} \ln(t) \quad (12)$$

where  $q_e$  and  $q_t$  (mg/g) are the amount of MB adsorbed per mass of adsorbent at equilibrium and time  $t$  (min), respectively,  $K_1$  ( $\text{min}^{-1}$ ) is the adsorption rate constant for pseudo-first-order model,  $K_2$  (g/mg min) is the rate constant of second order model,  $\alpha$  initial adsorption rate (mg/g min) and  $\beta$  desorption constant (g/mg).

### 3. Results and discussion

#### 3.1. Biochar characterization

The dye removal efficiency of adsorbents is likely related to the porosity and the functional groups of the adsorbent. The kind and nature of the functional groups may denote the adsorption capacity and pollutant removal efficiency of the prepared adsorbent. Fig. 2 presents FTIR spectra for the functional groups on the *P. excelsa* biochar before and after the adsorption of MB.

FTIR spectra showed common functional groups on the surface of *P. excelsa* biochar. Before the adsorption process, the band at 3,300–3,500  $\text{cm}^{-1}$  is related to the stretching of –OH [28,29], the deformation band at 2,900–3,100  $\text{cm}^{-1}$  is associated with the C–H bond (alkyl, aliphatic and aromatic groups). Peak at 1,691  $\text{cm}^{-1}$  can be associated to the elongation of C–O bonds in nonionic carboxylic groups (–COOH, –COOCH<sub>3</sub>) [30]. Peaks found between 1,050 and 600  $\text{cm}^{-1}$  are associated to C–OH, C–O–C and aromatic bonds [31]. After adsorption, many peaks intensity increased. The –OH bond at 3,200–3,700  $\text{cm}^{-1}$  was intensified may be due to the hydrated MB molecules [32]. The peak at 2,900–3,100  $\text{cm}^{-1}$  attributed to C–H stretching modes of the methyl groups in MB. Also, strengthened peaks at 875 and 811  $\text{cm}^{-1}$  attributed to C–H stretching in the benzene rings of MB molecules [32]. This indicated truly the adsorption of MB onto *P. excelsa*

biochar. After adsorption, there has been some shift of these peaks as a result of likely participation of the functional groups present on the adsorbent [30,33].

Figs. 3a and b present SEM images of *P. excelsa* biochar at different magnifications before adsorption. The pyrolysis process developed pores on the *P. excelsa* biochar surface with different pore sizes suggesting that *P. excelsa* biochar had a porous structure. The structure had a honeycomb-like porous network [34], which may be proper for the adsorption of MB molecules. The BET results suggested a specific surface area of 86.3  $\text{m}^2/\text{g}$ , average pore volume of 0.0312  $\text{cc}/\text{g}$  and average pore diameter of 2.4 nm for *P. excelsa* biochar, respectively.

#### 3.2. Contact time effect

Fig. 4 presents the dye removal percentage vs. time. The initial MB concentration is 25 mg/L and biochar dose is 0.2 g per 100 mL solution at pH 7. As shown in Fig. 4, the removal percentage increased with an increased contact

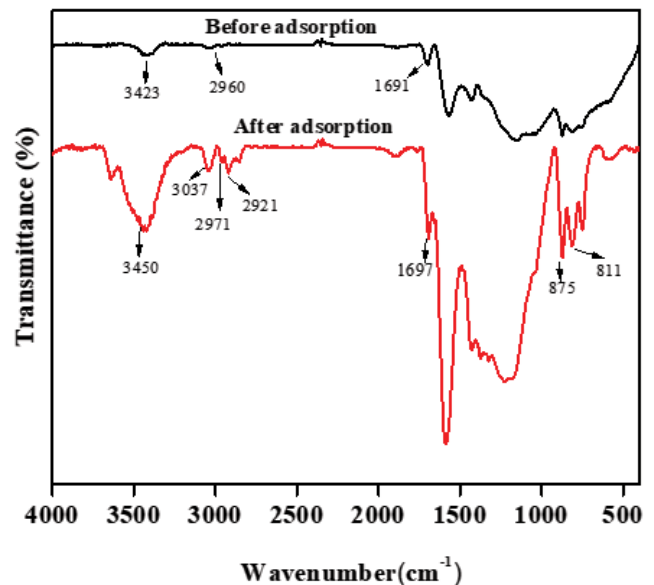


Fig. 2. FTIR spectra for *P. excelsa* biochar before and after adsorption.

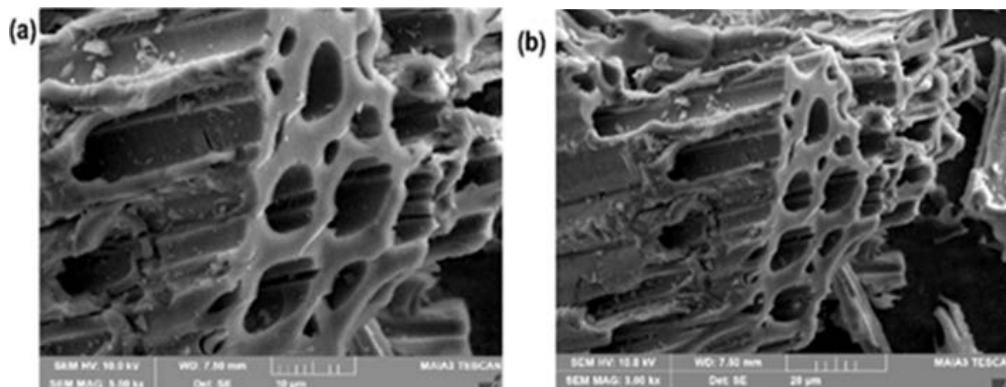


Fig. 3. (a) 5,000X and (b) 3,000X SEM image of *Parinari excelsa* biochar before MB adsorption.

time and then the maximum value was achieved finally. The rate of dye removal was rapid within 30 min as a result of vacant adsorption sites on the adsorbent. However, the removal percentage gradually slowed down before achieving equilibrium [35]. This was because there was a lot of empty adsorption sites on the adsorbent at the initial stage and the available adsorption sites became less after a period. It can be concluded that prolonging the treatment time will not further improve the MB removal significantly. The dye removal percentage reached 97% within 720 min of contact time. Similar trend has been reported on the removal efficiency of MB dye onto meranti sawdust [36].

3.3. Initial dye concentration effect

Initial dye concentration has a significant effect on adsorption equilibrium. The effect of initial dye concentrations ranging from 35 to 75 mg/L was examined by stirring 100 mL MB aqueous solution with 0.2 g of *P. excelsa* biochar for 24 h, and the results are presented in Fig. 5. The MB removal percentage decreased from 85% to 63% as the MB concentration increased from 35 to 75 mg/L. This

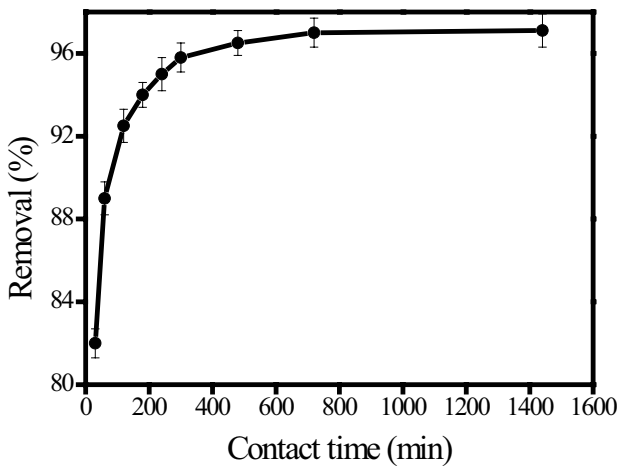


Fig. 4. Effect of contact time on MB removal.

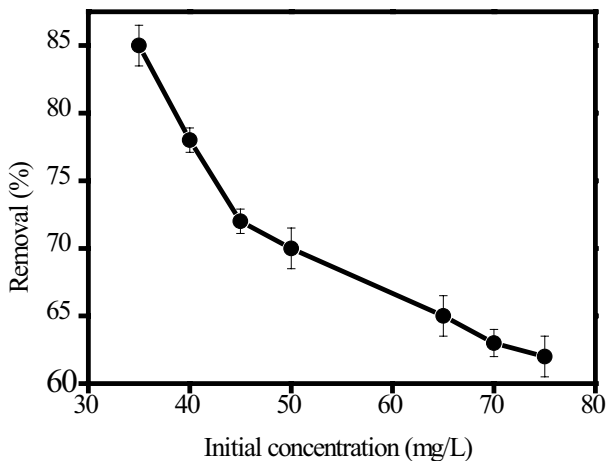


Fig. 5. Effect of initial dye concentration on removal efficiency of MB.

can be attributed to relatively less MB molecules for adsorption at lower MB concentrations under the same adsorbent dosage and also usually observed by others [37,38].

3.4. Adsorbent dose effect

The adsorbent dosage is a significant process parameter to be considered for batch adsorption studies. Fig. 6 shows that MB removal percentages increase with increasing adsorbent dosages. For adsorbent dose increased from 0.04 to 0.2 g/L, the removal percentages increased from 19% to 97% with 25 mg/L initial MB concentration. Beyond 0.16 g adsorbent dose, though slight increase in MB removal was also observed with more dosages, the optimum biochar dose was determined to be 0.16 g. At higher biochar dose to MB concentration ratios, there were higher removal percentages in MB concentration. This was a result of abundant vacant active sites compared with MB concentration [28]. Normally keeping the initial dye concentration constant and then increasing the adsorbent dosage provides a larger surface area and more adsorption sites, the dye uptake is then improved [38].

3.5. Salt concentration effect

The salt concentration may have significant effect on adsorption process. The effect of the MB adsorption was determined by mixing 100 mL MB aqueous solution (35mg/L) with 0.16 g biochar and varied sodium chloride amount in the range of 0.1–1.0 g. The results are presented in Fig. 7. The results showed that adsorption of MB increased with increasing concentration of sodium chloride. As shown in Fig. 7, the dye removal efficiency increased from 86% to 97% for sodium chloride ranging from 0.1 to 1.0 g. It shall be noted the removal efficiency here was obtained with initial MB concentration of 35 mg/L. Similar results can also be found in other reports [17,39].

3.6. pH effect

pH influences the adsorption of dyes by regulating the availability of active sites on adsorbents and ionization of

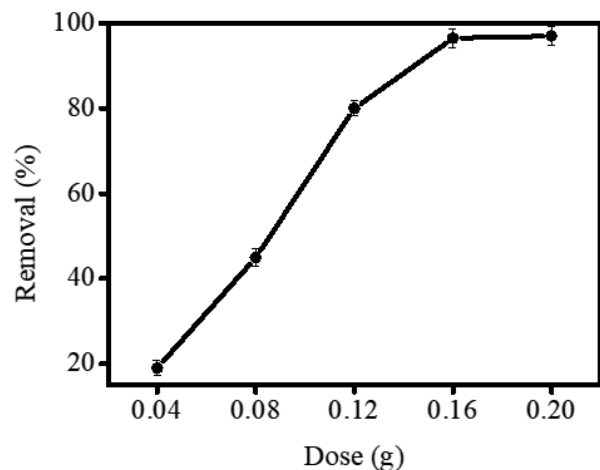


Fig. 6. Effect of adsorbent dose on the removal of MB.

adsorbates [40]. In this study, the pH of MB aqueous solution was examined in the range of 3–10 at a constant adsorbent dosage of 0.16 g per 100 mL solution with initial MB concentration of 30 mg/L. The results are presented in Fig. 8. It can be observed that the optimum condition for the highest MB removal was at pH 10 [41]. From Fig. 8, it can be observed that the removal efficiency for solution pH 3 and 10 was 85% and 99%, respectively. It shall be noted the removal efficiency here was obtained with initial MB concentration of 30 mg/L. In acidic medium, the adsorption of the MB was low due to the presence of abundant  $H^+$  ions competing with MB cations for the adsorption sites [10]. Other researchers had reported similar results for the uptake of MB onto broad beans peels, pine corn biomass [26,42] and hydrothermal carbonized and sodium hydroxide activated palm date seed [43].

### 3.7. Adsorption isotherm

The adsorption isotherm explains the nature of the interaction between adsorbate (MB) and the adsorbent. The experimental data were fitted with (i) Langmuir, (ii) Freundlich, (iii) Temkin and (iv) Dubinin–Radushkevich (D-R) adsorption isotherms. The fitting plots are shown

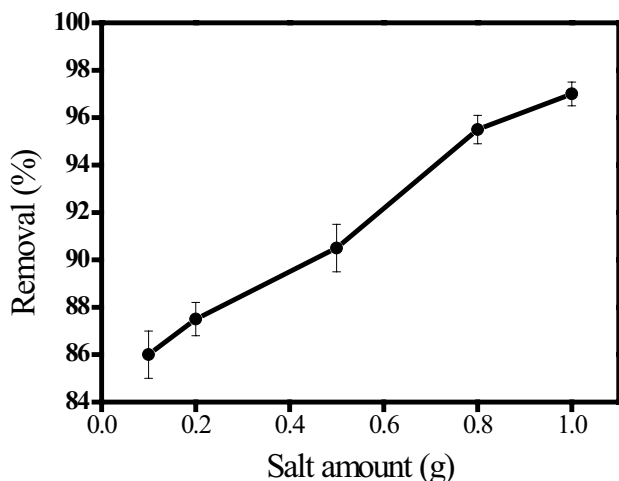


Fig. 7. Effect of salt concentration on dye removal in aqueous solution.

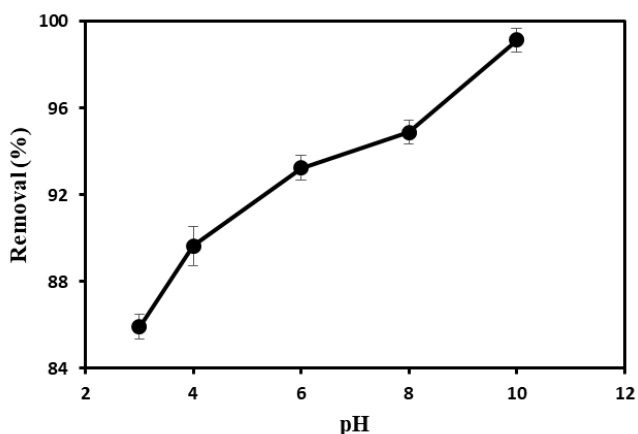


Fig. 8. Effect of pH on the adsorption of MB on *Parinari excelsa*.

in Figs. 9, S1 and S2. The values of the various isotherm parameters were obtained, respectively, from the linear correlations between (i)  $C_e/q_e$  vs.  $C_e$ , (ii)  $\log q_e$  vs.  $\log C_e$ , (iii)  $q_e$  vs.  $\ln C_e$  and (iv)  $\ln q_e$  vs.  $\epsilon^2$ . The adsorption isotherm parameters along with the correlation coefficients ( $R^2$ ) are listed in Table 1, respectively.

Fig. 9 presents the Langmuir (Fig. 9a) and Freundlich fit (Fig. 9b) of the experimental data and the separation factor  $R_L$  vs. initial concentrations (Fig. 9c). The Langmuir fit was the best fit model due to the highest value of the regression coefficient ( $R^2 = 0.931$ ). Also, the calculated monolayer adsorption capacity ( $Q_0$ ) was 30 mg/g for the Langmuir isotherm, which was in close agreement with the experimental value. The separation factor ( $R_L$ ) for the adsorption of MB onto *P. excelsa* biochar for different experimental concentrations of 35–75 mg/L was 0.203–0.106. The plot of the separation factor  $R_L$  vs. the initial concentration is shown in Fig. 9c. Here,  $R_L$  is lower than 1 and decreases with increasing MB concentrations. This confirmed that adsorption was enhanced at higher concentration [44–46]. In Freundlich fit,  $1/n$  is lower than 1 (shown in Table 1), which also confirms the favorable adsorption.

From the regression coefficients, the MB adsorption on *P. excelsa* biochar cannot be exactly described by Temkin and D-R isotherm models. However some of the fitting parameters still can give useful information. As shown in Table 1, the positive Temkin's constant  $b_T$  indicates that the adsorption is exothermic. The mean adsorption free energy of 2.1 kJ/mol as calculated from D-R model indicates that the adsorption is physical adsorption due to the low adsorption free energy value ( $<8$  kJ/mol).

### 3.8. Adsorption kinetics

Adsorption kinetics study the adsorption rates at different time during adsorption process. In this study, the pseudo-first-order, pseudo-second-order and Elovich kinetic models were tested for the experimental data. For the experiments, *P. excelsa* biochar of 0.2 g was stirred in 100 mL aqueous solution with 25 mg/L MB at a contact time ranging from 30 to 1,440 min at 30°C and pH 7. The amount of MB adsorbed per mass of adsorbent at equilibrium was measured to be 12.6 mg/g under the above conditions. The model fits were shown in Fig. 10.

Fig. 10a shows the pseudo-first-order fit of MB adsorption onto *P. excelsa*. The kinetic constant  $K_1$  of  $0.537 \text{ min}^{-1}$  and  $q_e$  of 1.093 mg/g are calculated from the slope and intercept, respectively and presented in Table 2. The correlation coefficient  $R^2$  of the pseudo-first-order is equal to 0.810. The pseudo-second-order fit is shown in Fig. 10b, also with  $R^2$  and other model parameters given in Table 2. The  $R^2$  for the pseudo-second-order kinetic model was 0.999. Also, the calculated value  $q_e$  of 12.5 mg/g for the pseudo-second-order was strongly in agreement with the experimental value of 12.6 mg/g. The Elovich kinetic model fit is presented in Fig. 10c. The model constants  $\alpha$  and  $\beta$  were calculated from the intercept and the slope, respectively and presented in Table 2. The  $R^2$  of 0.666 is less than those for both pseudo-first-order and pseudo-second-order. Therefore, the adsorption process can be appropriately described by pseudo-second-order kinetic model.

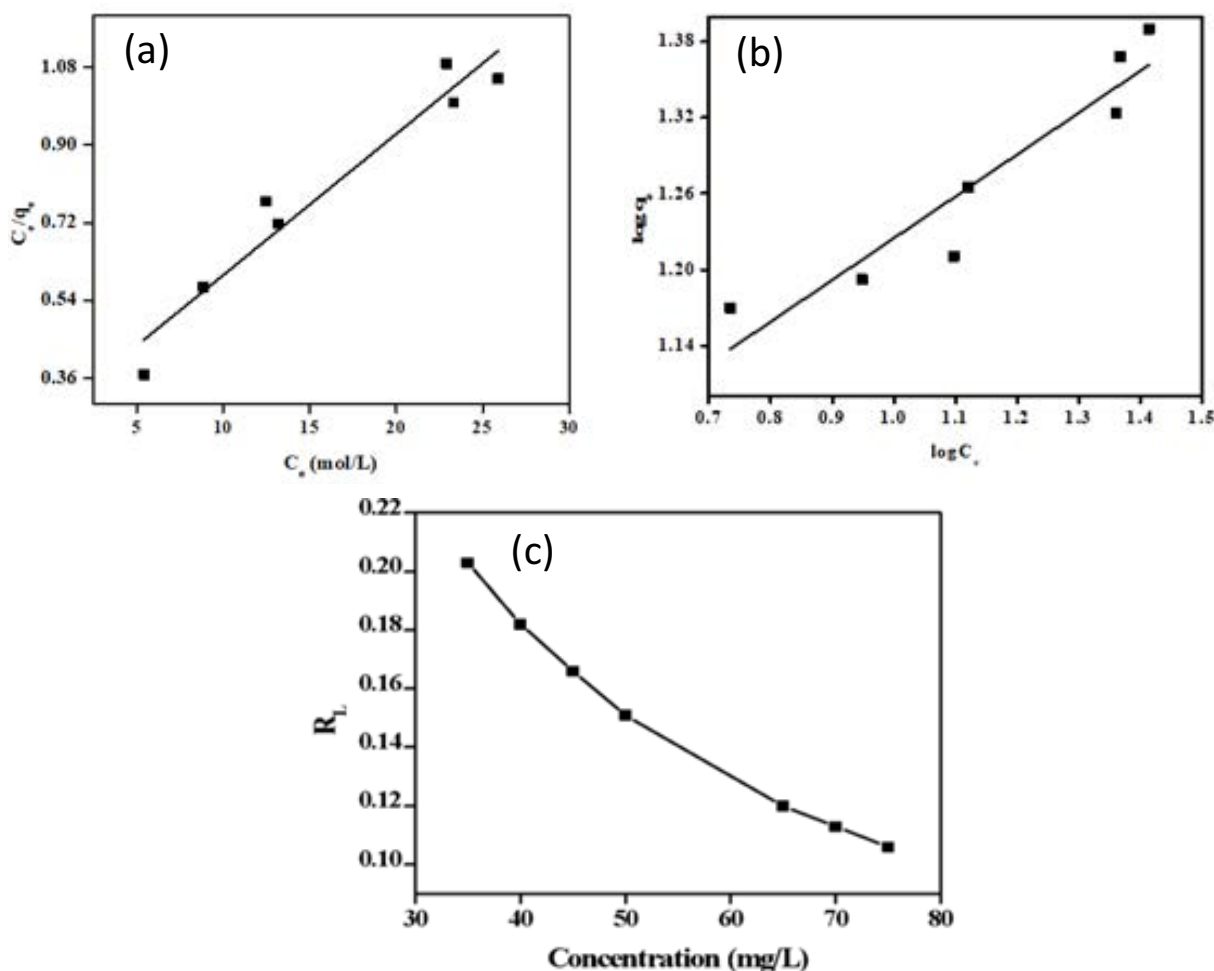


Fig. 9. Different isotherm fit for MB adsorption (a) Langmuir, (b) Freundlich and (c) separation factor vs. initial MB concentration.

Table 1  
Adsorption isotherm parameters for Langmuir, Freundlich, Temkin and D-R fits

Adsorbent	Model	Parameter 1	Parameter 2	Parameter 3	R <sup>2</sup>
<i>P. excelsa</i> biochar	Langmuir	Q <sub>0</sub> = 30 mg/g	b = 0.11 L/mg	–	0.931
	Freundlich	1/n = 0.33	K <sub>F</sub> = 2.44 mg/g	–	0.866
	Temkin	b <sub>T</sub> = 12,117 mg/L	a <sub>T</sub> = 803 L/g	–	0.832
	D-R	q <sub>s</sub> = 2.4 mg/g	K = 0.11 (mol/kJ) <sup>2</sup>	E = 2.1 kJ/mol	0.667

4. Performance evaluation

Table 3 lists the adsorption capacity (Q<sub>0</sub>) for various adsorbents in literatures with similar adsorption conditions. Studies show that Q<sub>0</sub> for MB adsorption on other biochars is often less than that on *P. excelsa* biochar. Some reports involved the surface synthesis of biochar, which can enhance its adsorptive capacities. But the surface synthesis involved complex and expensive processes which may contribute to higher cost of the process [44,45,47] compared with this study. In our view, *P. excelsa* biochar can serve as an alternative to commercial activated carbon in respect to the environmental issues.

5. Conclusions

This study showed that biochar from *P. excelsa* can effectively remove MB from simulated MB wastewater. Isotherm analysis showed that Langmuir model could best describe the adsorption equilibrium. The adsorption kinetics was best fitted by the pseudo-second-order kinetic model. The result indicated that *P. excelsa* biochar was a promising adsorbent material in dye removal. The amount of dye adsorbed increased with increasing dye concentration, salt concentration and solution pH.

This is a valuable addition to wood biomass in Sierra Leone, additional revenue to rural farmers. Biochar produced

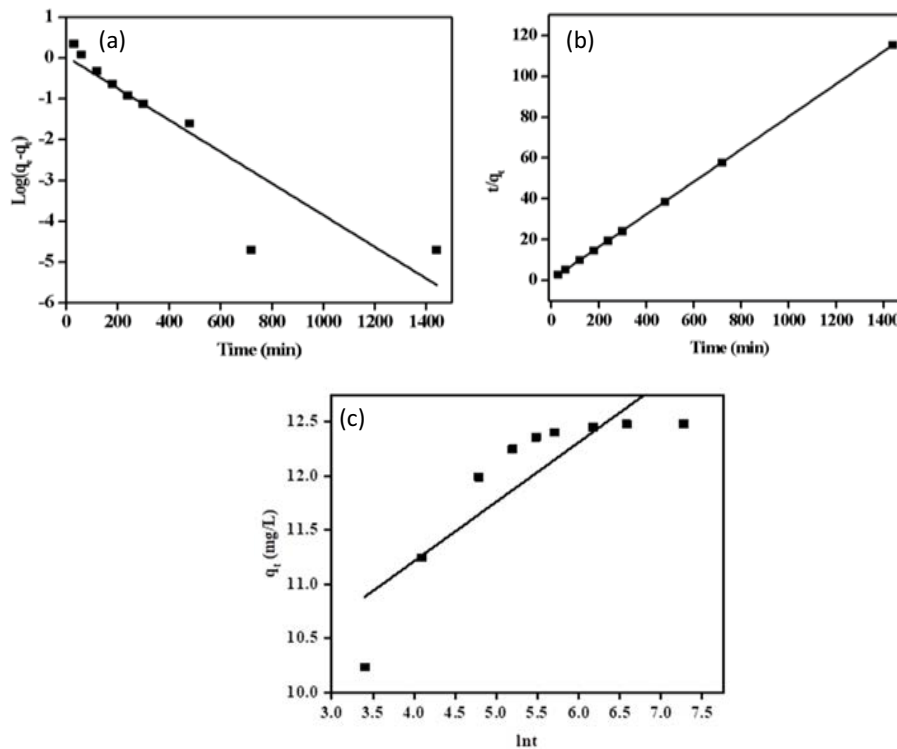


Fig. 10. Pseudo-first-order (a), pseudo-second-order (b) and Elovich (c) kinetic models fit.

Table 2  
Adsorption kinetic parameters for different model fits

Adsorbent	Model	Parameter 1	Parameter 2	R <sup>2</sup>
<i>P. excelsa</i> biochar	Pseudo-first-order	Calculated $q_e = 1.093$ mg/g	$K_1 = 0.537$ min <sup>-1</sup>	0.81
	Pseudo-second-order	Calculated $q_e = 12.5$ mg/g	$K_2 = 1.016$ g/mg min	0.999
	Elovich	$\alpha = 66,270,688$	$\beta = 1.819$	0.716

Table 3  
Comparison of MB adsorption capacities for different adsorbents

Adsorbent	Adsorption capacity (mg/g)	Reference No.
Weeds based char	39.68	[48]
Peanut stick biochar	2.54	[49]
Untreated sawdust	4.58	[50]
Pinewood biochar	16.3	[51]
Paper biochar	1.66	[51]
Pig manure biochar	25	[51]
Coir pitch carbon	5.87	[52]
Banana peel	15.9	[53]
<i>P. excelsa</i> biochar	30.0	This study

from *P. excelsa* can be used by local farmers to treat their drinking waters. Also, local industries can treat their color effluents before discharging into the environment using *P. excelsa* biochar at low costs, compared with the conventional activated carbon.

### Acknowledgements

The authors would like to thank the key research and development projects of Shaanxi province, China (2018GY097 & 2018SF383), for the financial support.

### References

- [1] V. Vadivelan, K.V. Kumar, Equilibrium, kinetics, mechanism, and process design for the sorption of methylene blue onto rice husk, *J. Colloid Interface Sci.*, 286 (2005) 90–100.
- [2] A. Hussam, A.K. Munir, A simple and effective arsenic filter based on composite iron matrix: development and deployment studies for groundwater of Bangladesh, *J. Environ. Sci. Health A*, 42 (2007) 1869–1878.
- [3] J. Okello, P. Ssegawa, Medicinal plants used by communities of Ngai Subcounty, Apac District, northern Uganda, *Afr. J. Ecol.*, 45 (2007) 76–83.
- [4] M. Khayznikov, K. Hemachandra, R. Pandit, A. Kumar, P. Wang, C.J. Glueck, Statin intolerance because of myalgia, myositis, myopathy, or myonecrosis can in most cases be safely resolved by vitamin D supplementation, *North Am. J. Med. Sci.*, 7 (2015) 86–93.
- [5] A.A. Said, A.A. Aly, M.M.E. Abd, S.A. Soliman, A.A.E. Abd, V. Helmeq, M.N. Goda, Application of modified bagasse

- as a biosorbent for reactive dyes removal from industrial wastewater, *J. Water Resour. Prot.*, 5 (2013) 10–17.
- [6] T. Subasioglu, I.S. Bilkay, Determination of biosorption conditions of methyl orange by *Humicola fuscoatra*, *J. Sci. Ind. Res.*, 68 (2009) 1075–1077.
- [7] W.D. Heiss, M. Huber, G.R. Fink, K. Herholz, U. Pietrzyk, R. Wagner, K. Wienhard, Progressive derangement of periinfarct viable tissue in ischemic stroke, *J. Cereb. Blood Flow Metab.*, 12 (1992) 193–203.
- [8] S.E. Comstock, T.H. Boyer, Combined magnetic ion exchange and cation exchange for removal of DOC and hardness, *Chem. Eng. J.*, 241 (2014) 366–375.
- [9] S. Kumar, C. Guria, A. Mandal, Synthesis, characterization and performance studies of polysulfone/bentonite nanoparticles mixed-matrix ultra-filtration membranes using oil field produced water, *Sep. Purif. Technol.*, 150 (2015) 145–158.
- [10] D. Hu, H. Wu, Y. Li, Positively charged ultrafiltration membranes fabricated via graft polymerization combined with crosslinking and branching for textile wastewater treatment, *Sep. Purif. Technol.*, 264 (2021) 118469.
- [11] G. Ciardelli, L. Corsi, M. Marucci, Membrane separation for wastewater reuse in the textile industry, *Resour. Conserv. Recycl.*, 31 (2001) 189–197.
- [12] M.I. Aguilar, J. Saez, M. Liorens, A. Soler, J.F. Ortuno, Nutrient removal and sludge production in the coagulation–flocculation process, *Water Res.*, 36 (2002) 2910–2919.
- [13] R. Gong, X. Zhang, H. Liu, Y. Sun, B. Liu, Uptake of cationic dyes from aqueous solution by biosorption onto granular kohlrabi peel, *Bioresour. Technol.*, 98 (2007) 1319–1323.
- [14] G. Crini, Non-conventional low-cost adsorbents for dye removal: a review, *Bioresour. Technol.*, 97 (2006) 1061–1085.
- [15] G.M. Gadd, Biosorption: critical review of scientific rationale, environmental importance and significance for pollution treatment, *J. Chem. Technol. Biotechnol.*, 84 (2009) 13–28.
- [16] W. Gwenz, N. Chaukura, C. Noubactep, F.N. Mukome, Biochar-based water treatment systems as a potential low-cost and sustainable technology for clean water provision, *J. Environ. Manage.*, 197 (2017) 732–749.
- [17] M.E. Mahmoud, G.M. Nabil, N.M. El-Mallah, H.I. Bassiouny, S. Kumar, T.M. Abdel-Fattah, Kinetics, isotherm, and thermodynamic studies of the adsorption of reactive red 195A dye from water by modified Switchgrass biochar adsorbent, *J. Ind. Eng. Chem.*, 37 (2016) 156–167.
- [18] D.D. Sewu, P. Boakye, S.H. Woo, Highly efficient adsorption of cationic dye by biochar produced with Korean cabbage waste, *Bioresour. Technol.*, 224 (2017) 206–213.
- [19] A. Shukla, Y.H. Zhang, P. Dubey, J.L. Margrave, S.S. Shukla, The role of sawdust in the removal of unwanted materials from water, *J. Hazard. Mater.*, 95 (2002) 137–152.
- [20] L. Sun, S. Wan, W. Luo, Biochars prepared from anaerobic digestion residue, palm bark, and eucalyptus for adsorption of cationic methylene blue dye: characterization, equilibrium, and kinetic studies, *Bioresour. Technol.*, 140 (2013) 406–413.
- [21] N. Wibowo, L. Setyadi, D. Wibowo, J. Setiawan, S. Ismadi, Adsorption of benzene and toluene from aqueous solutions onto activated carbon and its acid and heat treated forms: influence of surface chemistry on adsorption, *J. Hazard. Mater.*, 146 (2007) 237–242.
- [22] G. Enaime, K. Ennaciri, A. Ounas, A. Baaoui, A. Yaacoubi, Preparation and characterization of activated carbons from olive wastes by physical and chemical activation: application to indigo carmine adsorption, *J. Mater. Environ. Sci.*, 8 (2017) 4125–4137.
- [23] M.A. Islam, M. Auta, G. Kabir, B.H. Hameed, A thermogravimetric analysis of the combustion kinetics of karanja (*Pongamia pinnata*) fruit hulls char, *Bioresour. Technol.*, 200 (2016) 335–341.
- [24] M.M. Keiluweit, P.S. Nico, M.G. Johnson, M. Kleber, Dynamic molecular structure of plant biomass derived black carbon (biochar), *Environ. Sci. Technol.*, 44 (2010) 1247–1253.
- [25] M. Inyang, B. Gao, A. Zimmerman, M. Zhang, H. Chen, Synthesis, characterization, and dye sorption ability of carbon nanotube–biochar nanocomposites, *Chem. Eng. J.*, 236 (2014) 39–46.
- [26] B.H. Hameed, A.T.M. Din, A.L. Ahmad, Adsorption of methylene blue onto bamboo-based activated carbon: kinetics and equilibrium studies, *J. Hazard. Mater.*, 141 (2007) 819–825.
- [27] Z. Cheng, L. Zhang, X. Guo, X. Jiang, T. Li, Adsorption behavior of direct red 80 and congo red onto activated carbon/surfactant: process optimization, kinetics and equilibrium, *Spectrochim. Acta A*, 137 (2015) 1126–1143.
- [28] G.B. Kankilic, A.U. Metin, I. Tuzun, *Phragmites australis*: an alternative biosorbent for basic dye removal, *Ecol. Eng.*, 86 (2016) 85–94.
- [29] P. Das Saha, S. Chakraborty, S. Chowdhury, Batch and continuous (fixed-bed column) biosorption of crystal violet by *Artocarpus heterophyllus* (jackfruit) leaf powder, *Colloid Surf. B*, 92 (2012) 262–270.
- [30] X. Pang, L. Sellaoui, D.S.P. Franco, M.S. Netto, J. Georgin, G.L. Dotto, M.K. Abu Shayeb, H. Belmabrouk, A. Bonilla-Petriciolet, Z.C. Li, Preparation and characterization of a novel mountain soursop seeds powder adsorbent and its application for the removal of crystal violet and methylene blue from aqueous solutions, *Chem. Eng. J.*, 391 (2019) 123617.
- [31] S. Roman, N.J.M. Valente, B. Ledesma, J.F. Gonzalez, C. Laginhas, M.M. Titirici, Production of low-cost adsorbents with tunable surface chemistry by conjunction of hydrothermal carbonization and activation processes, *Microporous Mesoporous Mater.*, 165 (2013) 127–133.
- [32] Y. Zhang, J.T. Wang, L. Tang, Structure analysis of methylene blue, *Proc. Clin. Med.*, 19 (2010) 941–943.
- [33] D. Guo, Y. Li, B. Cui, M. Hu, S. Luo, B. Ji, Y. Liu, Natural adsorption of methylene blue by waste fallen leaves of Magnoliaceae and its repeated thermal regeneration for reuse, *J. Cleaner Prod.*, 267 (2020) 121903.
- [34] L.A. Jonas, J.A. Rehrmann, The rate of gas adsorption by activated carbon, *Carbon*, 12 (1974) 95–101.
- [35] D.K. Mahmoud, M.A.M. Salleh, W.A.W.A. Karim, A. Idris, Z.Z. Abidin, Batch adsorption of basic dye using acid treated kenaf fibre char: equilibrium, kinetic and thermodynamic studies, *Chem. Eng. J.*, 181 (2012) 449–457.
- [36] K.D. Belaid, S. Kacha, M. Kameche, Z. Derriche, Adsorption kinetics of some textile dyes onto granular activated carbon, *J. Environ. Chem. Eng.*, 3 (2013) 496–503.
- [37] S. Guiza, M. Bagane, A.H. Al-Soudani, H.B. Amore, Adsorption of basic dyes onto natural clay, *Adsorpt. Sci. Technol.*, 22 (2004) 245–255.
- [38] D. Lin, F. Wu, Y. Hu, T. Zhang, C. Liu, Y. Hu, Z.H. Xue, H. Han, Z.H. Ko, Adsorption of dye by waste black tea powder: parameters, kinetic, equilibrium, and thermodynamic studies, *J. Chem.*, 2020 (2020) 5431046.
- [39] Y. Kuang, X. Zhang, S. Zhou, Adsorption of methylene blue in water onto activated carbon by surfactant modification, *Water*, 12 (2020) 1–19.
- [40] A. Afkhami, R. Moosavi, Adsorptive removal of Congo red, a carcinogenic textile dye, from aqueous solutions by maghemite nanoparticles, *J. Hazard. Mater.*, 174 (2010) 398–403.
- [41] A. Ouldoumna, L. Reinert, N. Benderdouche, B. Bestani, L. Duclaux, Characterization and application of three novel biosorbents “*Eucalyptus globulus*”, *Cynara cardunculus*”, and *Prunus cerasifera*” to dye removal, *Desal. Wat. Treat.*, 51 (2013) 3527–3538.
- [42] T.K. Sen, S. Afroze, H.M. Ang, Equilibrium, kinetics and mechanism of removal of methylene blue from aqueous solution by adsorption onto pine cone biomass of *Pinus radiata*, *Water Air Soil Pollut.*, 218 (2011) 499–515.
- [43] M.A. Islam, I.A.W. Tan, A. Benhouria, M. Asif, B.H. Hameed, Mesoporous and adsorptive properties of palm date seed activated carbon prepared via sequential hydrothermal carbonization and sodium hydroxide activation, *Chem. Eng. J.*, 270 (2015) 187–195.
- [44] G.O. El-Sayed, Removal of methylene blue and crystal violet from aqueous solutions by palm kernel fiber, *Desalination*, 272 (2011) 225–232.

- [45] S. Chatterjee, M.W. Lee, S.H. Woo, Adsorption of Congo red by chitosan hydrogel beads impregnated with carbon nanotubes, *Bioresour. Technol.*, 101 (2010) 1800–1806.
- [46] B.H. Hameed, Spent tea leaves: a new non-conventional and low-cost adsorbent for removal of basic dye from aqueous solutions, *J. Hazard. Mater.*, 161 (2009) 753–759.
- [47] A.M. Vargas, A.L. Cazetta, M.H. Kunita, T.L. Silva, V.C. Almeida, Adsorption of methylene blue on activated carbon produced from flamboyant pods (*Delonix regia*): study of adsorption isotherms and kinetic models, *Chem. Eng. J.*, 168 (2011) 722–730.
- [48] F. Guzel, H. Saygili, G.A. Saygili, F. Koyuncu, C. Yilmaz, Optimal oxidation with nitric acid of biochar derived from pyrolysis of weeds and its application in removal of hazardous dye methylene blue from aqueous solution, *J. Cleaner Prod.*, 144 (2017) 260–265.
- [49] M. Ghaedi, A.G. Nasab, S. Khodadoust, M. Rajabi, S. Azizian, Application of activated carbon as adsorbents for efficient removal of methylene blue: kinetics and equilibrium study, *J. Ind. Eng. Chem.*, 20 (2014) 2317–2324.
- [50] S. Banerjee, M.C. Chattopadhyaya, V. Srivastava, Y.C. Sharma, Adsorption studies of methylene blue onto activated saw dust: kinetics, equilibrium, and thermodynamic studies, *Environ. Prog. Sustain. Energy*, 33 (2014) 790–799.
- [51] L. Lonappan, T. Rouissi, R.K. Das, S.K. Brar, A.A. Ramirez, M. Verma, R.Y. Surampalli, J.R. Valero, Adsorption of methylene blue on biochar microparticles derived from different waste materials, *Waste Manage.*, 49 (2016) 537–544.
- [52] D. Kavitha, C. Namasivayam, Experimental and kinetic studies on methylene blue adsorption by coir pith carbon, *Bioresour. Technol.*, 98 (2007) 14–21.
- [53] G. Annadurai, R.S. Juang, D.J. Lee, Use of cellulose-based wastes for adsorption of dyes from aqueous solutions, *J. Hazard. Mater.*, 92 (2002) 263–274.

### Supplementary information

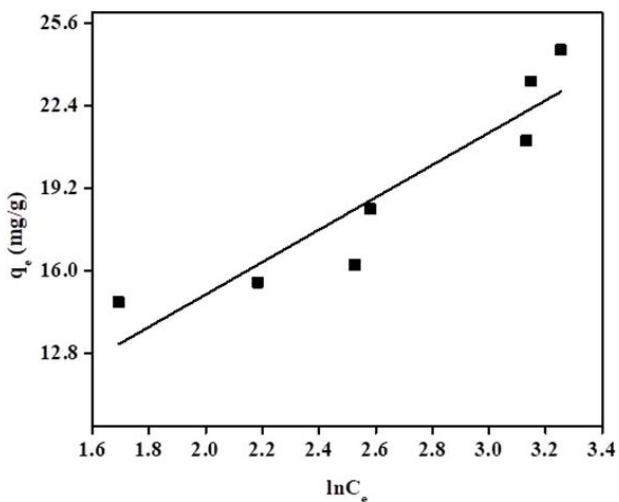


Fig. S1. Temkin isotherm fit.

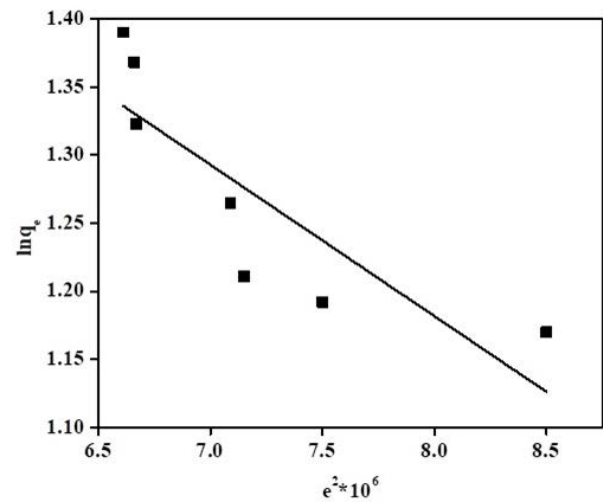


Fig. S2. D-R isotherm fit.